

# THE ALKALI FELDSPARS: II. A SIMPLE X-RAY TECHNIQUE FOR THE STUDY OF ALKALI FELDSPARS

J. V. SMITH AND W. S. MACKENZIE, *Geophysical Laboratory,  
Carnegie Institution of Washington, Washington, D.C.*

## ABSTRACT

A routine *x*-ray method has been developed for the study of alkali feldspars. From a single-crystal *x*-ray oscillation photograph the symmetry, twinning and unmixing may be seen at a glance. The reciprocal lattice angles  $\alpha^*$  and  $\gamma^*$  of triclinic phases, twinned on either the albite or pericline law, can be readily measured from the oscillation photograph by a new precision method.

## INTRODUCTION

X-ray powder methods are now in general use by mineralogists and petrologists for routine work of identification and determination of lattice parameters of known and unknown materials. Single-crystal techniques, however, are rarely used in routine work, and this is unfortunate because a wealth of information not accessible by powder methods can be obtained with little difficulty. This paper presents a single-crystal *x*-ray method for studying the lamellar structure of the alkali feldspars and for determining the reciprocal lattice angles  $\alpha^*$  and  $\gamma^*$  of a triclinic feldspar if it is twinned on either the albite or pericline law. The procedure for obtaining the *x*-ray photograph is hardly more difficult than the operation of the universal stage on a petrographic microscope, and the photograph may be interpreted at a glance. The reciprocal lattice angles  $\alpha^*$  and  $\gamma^*$  may be determined in 30 minutes with an accuracy of 3'–10' of arc. This *x*-ray method is thus ideally suited for a routine investigation of a large number of crystals. In order to encourage the use of this method by those mineralogists and petrologists whose knowledge of single-crystal work is elementary, the techniques will be described in some detail. Readers not familiar with single-crystal *x*-ray methods should consult a textbook such as Buerger (1942) or Henry, Lipson, and Wooster (1951).

Alkali feldspars are generally unmixed to two or more phases. The soda-rich phase or phases are triclinic and may have lattice angles similar to those of a low-temperature albite-oligoclase or to those of an orthoclase (a high-temperature alkali feldspar of composition between  $\text{Or}_{37}\text{Ab}_{63}$  and  $\text{Or}_0\text{Ab}_{100}$ ). The potash-rich phase or phases may be monoclinic (sanidine or orthoclase) or triclinic (microcline).\*

\* Laves (1952) has noted that a soda-rich high-temperature cryptoperthite may have a triclinic potash phase which is not microcline but potash feldspar forced to be triclinic by the predominant triclinic soda phase.

of the microperthites and cryptoperthites retain the morphology of a monoclinic feldspar from which they unmixed and often have optically monoclinic symmetry also. This pseudo-monoclinic symmetry may be used in the alignment of the crystals in the  $x$ -ray camera. From examination of various types of  $x$ -ray photographs of alkali feldspars we have found that a  $b$ -axis oscillation photograph with an oscillation angle of  $15^\circ$  is most suitable. A standard orientation has been adopted for each photograph, the crystal being set with the (001) cleavage parallel to the  $x$ -ray beam in the center of the oscillation.

Most alkali feldspar crystals have the (010) and (001) cleavages well developed. By use of the tele-microscope, fitted to some single-crystal  $x$ -ray cameras, or an auxiliary single-circle goniometer, the crystal may be set with an accuracy of  $1^\circ$ – $2^\circ$ . If the (010) and (001) cleavages are not visible, one of the standard  $x$ -ray setting techniques has to be used. With an orientation error of  $1^\circ$ – $2^\circ$  the resulting photograph is readily interpretable; however, if measurements are to be made from the photograph it is advisable to reduce the setting error below  $1^\circ$  using an  $x$ -ray setting technique.

The crystal setting is more difficult when the crystal consists solely of an albite twinned triclinic phase, as this gives two sets of layer lines at an angle of about  $4^\circ$ . The crystal may be set approximately by optical means, and after a preliminary  $x$ -ray photograph has been taken it may be adjusted on the arcs so that the two sets of layer lines are symmetrical about the equator of the photograph. A pericline twinned triclinic phase presents no difficulty since the  $b$ -axis is common to the twinned parts and there is only one set of layer lines.

A cylindrical camera has been used in preference to a flat plate camera because of the greater range in  $\theta$  and because it is an advantage to have straight layer lines. Filtered copper radiation was found to be the most convenient.

#### INTERPRETATION OF THE PHOTOGRAPH

In 1940, Chao and Taylor demonstrated that a simple crystallographic relationship exists between the differently oriented units of a microperthite. Others have confirmed the findings of Chao and Taylor and have amplified their results. The angular relations may be stated briefly as follows. A microperthite generally has a monoclinic potash phase whose orientation corresponds to the morphology of the crystal; thus the  $b$ -axis of the potash phase is coincident with the morphological  $b$ -axis of the crystal. The soda-rich phase or phases are triclinic and are twinned on the albite or pericline law. For the albite law the  $b^*$ -axis is common to the twinned individuals and almost always coincides with

the morphological  $b$ -axis; only two crystals have been found which violate this rule. For the pericline law the  $b$ -axis is common to the twinned individuals and coincides with the morphological  $b$ -axis. Sometimes albite and pericline twinning occur together and this may represent a single soda phase or two soda phases, one pericline twinned and the other albite twinned. Some low-temperature perthites have a triclinic potash phase twinned on the albite law or on both the albite and pericline law. In other cases the angular relations between the two triclinic units do not correspond with twinning on either the albite or pericline law.

In the  $x$ -ray oscillation photographs the potash-rich phases may be distinguished from the soda-rich phases since their reflections are

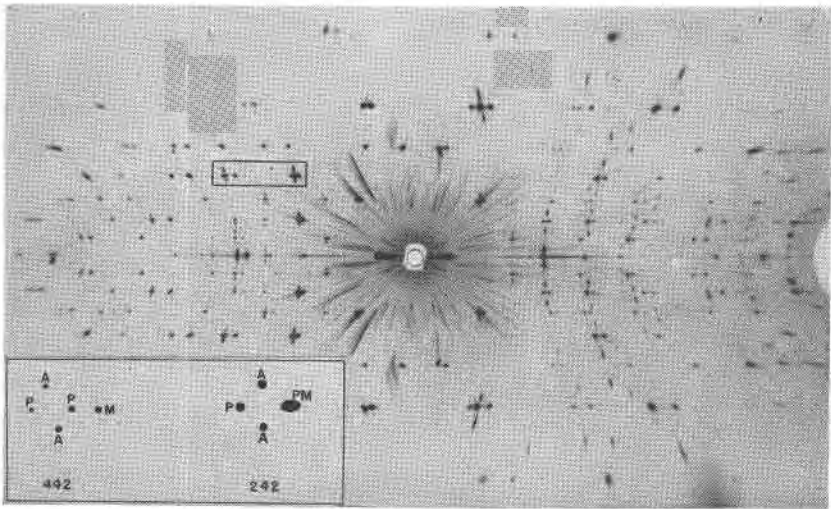


FIG. 1. Specimen  $O$ ,  $b$ -axis oscillation photograph with the  $x$ -ray beam parallel to (001) in the center of a  $15^\circ$  oscillation. The inset diagram in the bottom left-hand corner provides a key for the interpretation of the reflections enclosed in the small rectangle in the top left-hand corner.  $A$  and  $P$  denote the reflections from the albite- and pericline-twinned soda phase, respectively;  $M$  denotes the reflection from the potash phase.

generally nearer to the center of the photographs because of the differences between the lattice parameters of the two phases.

Figure 1 is a  $b$ -axis oscillation photograph of specimen  $O$ † which has a monoclinic potash phase together with a triclinic soda phase twinned according to the albite and pericline laws. It will be noticed that the potash reflections are usually closer to the center of the photograph and

† The three specimens mentioned in this paper are from a series of feldspars described by Spencer (1937). The letters  $O$ ,  $N$  and  $F$  used to denote these specimens are in accordance with the list in Spencer's paper.

that they are symmetrical about the zero layer line. The albite twinned soda reflections lie symmetrically above and below each layer line on curves of constant  $\xi$ , whereas the pericline twinned reflections lie on the layer lines (constant  $\zeta$ ). The separation of the pericline twinned reflections is zero on the equatorial layer line and increases with the order of the layer line. The common  $b^*$ -axis of the albite twinned reflections is

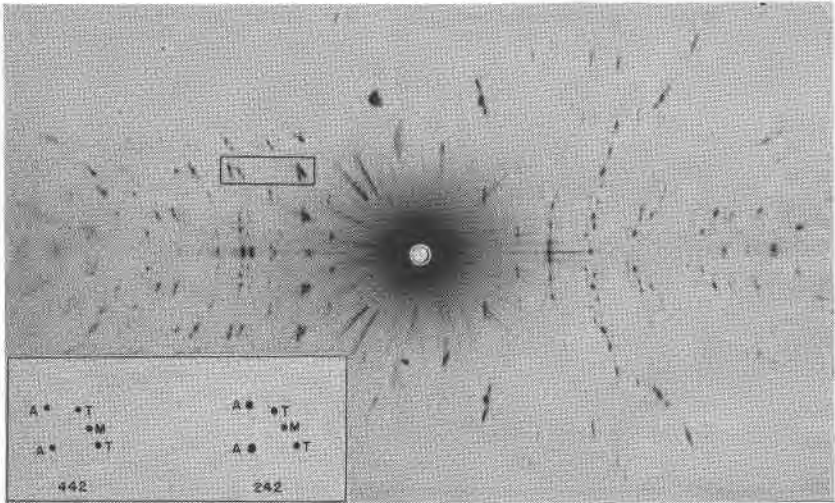


FIG. 2. Specimen *N*,  $b$ -axis oscillation photograph with the  $x$ -ray beam parallel to (001) in the center of a  $15^\circ$  oscillation. The inset diagram in the bottom left-hand corner provides a key for the interpretation of the reflections enclosed in the small rectangle in the top left-hand corner. *A* denotes the reflections from the albite-twinned soda phase; *M* and *T* denote the monoclinic and triclinic components of the potash phase, respectively.

coincident with the common  $b$ -axis of the pericline twinned reflections and with the  $b$ -axis of the monoclinic potash phase.

Figure 2 is an  $x$ -ray photograph of specimen *N*. The soda phase is albite twinned. The potash phase is represented by three reflections—the central spot is from a monoclinic component and the two outer reflections are from two triclinic components—which are angularly related in a complex manner. They are not twinned according to either the albite law or the pericline law, for the reflections lie neither on curves of constant  $\xi$  nor on curves of constant  $\zeta$ . The angular relations are given in the accompanying paper (MacKenzie and Smith).

Figure 3 is an  $x$ -ray photograph of a crystal of specimen *F* which was heated for 17 minutes at  $700^\circ$  C. to homogenize the soda and potash phases. It consists of a single monoclinic phase. The reflections in the

upper half of the photograph have been indexed and, since all photographs have been taken in the same orientation, the indices for the potash-rich phase in a perthitic feldspar may be obtained by comparison with this photograph. The indices of a soda-rich phase may also be obtained by comparison, but care is required in the high-angle regions because of the difference in lattice parameters between the soda and potash phases.

Untwinned homogeneous triclinic alkali feldspars are found and their x-ray photographs are very similar to those of monoclinic crystals so

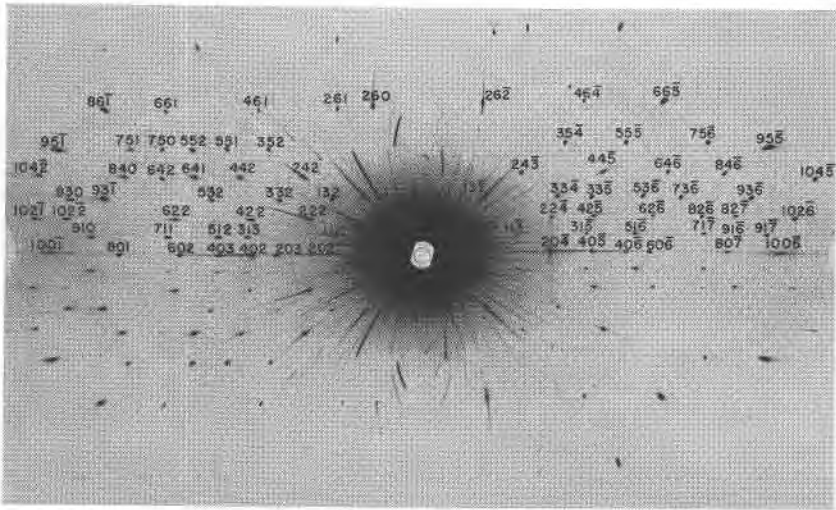


FIG. 3. Specimen *F*, heated 17 minutes at 700° C. to homogenize the soda and potash phases; *b*-axis oscillation photograph with the x-ray beam parallel to (001) in the center of a 15° oscillation. The reflections in the upper half of the photograph have been indexed, and for clarity these reflections have been replaced by small solid circles. The intensities of the reflections may be obtained from the lower half of the photograph. The composition of this specimen is  $Or_{78} sAb_{18} aAn_{2.3}$  (Spencer, 1937).

that great care must be taken before concluding that a feldspar is monoclinic. No confusion should arise for anorthoclase because there are large intensity differences between equivalent reflections above and below the zero layer line. For microclines, however, the intensity deviations are small, especially for the intermediate microclines. However, by careful comparison of intensities above and below the zero layer line (especially for reflections  $(71\bar{7})$  and  $(\bar{7}1\bar{7})$ ,  $(82\bar{7})$  and  $(\bar{8}2\bar{7})$ ) microcline can be distinguished from a monoclinic potash phase.

The reflections from alkali feldspars are often diffuse and are sometimes accompanied by diffuse streaks which join the sharp spots. The

diffuse streaks are caused by material whose structure is either strained or transitional between the structures which give the sharp reflections. Diffuse spots are caused by material which either is disordered or consists of very small blocks. These effects may be seen in Fig. 3 of the accompanying paper (MacKenzie and Smith).

As shown in the previous paper, knowledge of the angles  $\alpha^*$  and  $\gamma^*$  enables one to distinguish high-temperature from low-temperature soda-rich phases and also to distinguish a maximum from an intermediate microcline. The following section is devoted to a method for measuring the angles  $\alpha^*$  and  $\gamma^*$  from the standard  $b$ -axis oscillation photographs.

Bowen and Tuttle (1950) showed that the composition of a homogeneous high-temperature alkali feldspar can be determined from the spacing of the  $\bar{2}01$  reflection in a powder diffraction pattern. A simple method, based on the same principle, for determining the bulk composition of a single alkali feldspar crystal from a standard  $b$ -axis oscillation photograph will be described at a later date.

#### DETERMINATION OF $\alpha^*$ AND $\gamma^*$ FOR TWINNED TRICLINIC PHASES

Figure 4 shows the angular relations for albite and pericline twinning. In albite twinning the twin axis is normal to (010), i.e., the  $b^*$ -axis; in pericline twinning the twin axis is  $b$  and the  $b^*$ -axes do not coincide. In either case the reflections occur in pairs such that the twinned  $(\bar{h}k\bar{l})$ ‡ reflection is adjacent to the untwinned  $(hkl)$  reflection.

Using the formula which relates film coordinates  $\zeta$  and  $\xi$ , with the reciprocal lattice constants (Buerger, 1942),

$$\begin{aligned} \zeta^2 + \xi^2 = \frac{\lambda^2}{d_{hkl}^2} = & h^2 a^{*2} + k^2 b^{*2} + l^2 c^{*2} + 2kll^*c^* \cos \alpha^* \\ & + 2lhc^*a^* \cos \beta^* \\ & + 2hka^*b^* \cos \gamma^* \end{aligned}$$

where

$$a^* = \frac{\lambda}{d_{100}}, \quad b^* = \frac{\lambda}{d_{010}}, \quad \text{and} \quad c^* = \frac{\lambda}{d_{001}}$$

the following equation is obtained

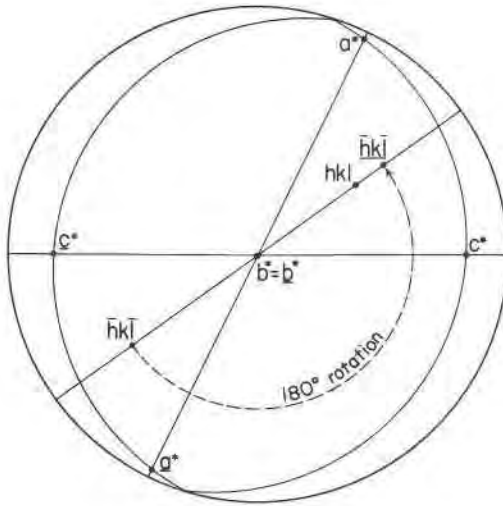
$$\zeta_{hkl}^2 + \xi_{hkl}^2 - \zeta_{\bar{h}k\bar{l}}^2 - \xi_{\bar{h}k\bar{l}}^2 = 4kb^*[lc \cos \alpha^* + la^* \cos \gamma^*]$$

For albite twinning  $\xi_{hkl} = \xi_{\bar{h}k\bar{l}}$  and for pericline twinning  $\zeta_{hkl} = \zeta_{\bar{h}k\bar{l}}$ . Therefore

$$\begin{aligned} 4kb^*[lc^* \cos \alpha^* + la^* \cos \gamma^*] &= \zeta_{hkl}^2 - \zeta_{\bar{h}k\bar{l}}^2 \quad (\text{albite twinning}) \\ &= \xi_{hkl}^2 - \xi_{\bar{h}k\bar{l}}^2 \quad (\text{pericline twinning}). \end{aligned}$$

‡ Indices of faces in the twinned position are underlined.

ALBITE TWINNING



PERICLINE TWINNING

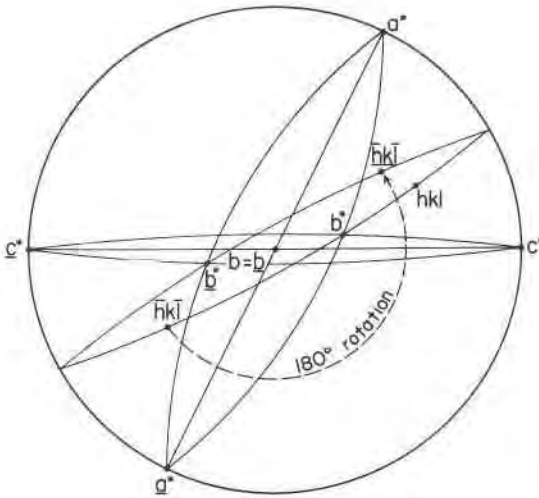


FIG. 4. The angular relations for albite and pericline twinning shown on stereographic projections. The angles  $\alpha^*$  and  $\gamma^*$  have been exaggerated.

By determining the values of

$$(\zeta^2_{hkl} - \zeta^2_{\bar{h}\bar{k}\bar{l}}) \quad \text{or} \quad (\xi^2_{hkl} - \xi^2_{\bar{h}\bar{k}\bar{l}})$$

for several sets of the paired reflections the values of  $c^* \cos \alpha^*$  and  $a^* \cos \gamma^*$  may be determined and hence  $\alpha^*$  and  $\gamma^*$  may be found.

The determination of  $\zeta$  and  $\xi$  from a Bernal chart is not sufficiently accurate for the present purpose, and the best method is to measure the displacement between the paired reflections using a viewing screen equipped with a vernier scale.

The equation for the albite twinning may be rewritten as

$$\begin{aligned} lc^* \cos \alpha^* + ha^* \cos \gamma^* &= \frac{1}{4kb^*} (\zeta_{hkl} + \zeta_{\bar{h}\bar{k}\bar{l}})(\zeta_{hkl} - \zeta_{\bar{h}\bar{k}\bar{l}}) \\ &= \frac{1}{2} (\zeta_{hkl} - \zeta_{\bar{h}\bar{k}\bar{l}}) \S \quad \text{for} \quad \zeta_{hkl} + \zeta_{\bar{h}\bar{k}\bar{l}} = 2kb^*. \end{aligned}$$

If a layer line  $\zeta$  in a cylindrical camera is displaced  $y$  mm. from the zero layer and

$$A = \frac{1}{2} \left( \frac{d\zeta}{dy} \right) \quad \text{at} \quad \zeta = \frac{1}{2} (\zeta_{hkl} + \zeta_{\bar{h}\bar{k}\bar{l}})$$

then if  $\Delta y_{hkl}$  is the separation of  $(hkl)$  and  $(\bar{h}\bar{k}\bar{l})$  measured *perpendicular* to the layer lines,

$$lc^* \cos \alpha^* + ha^* \cos \gamma^* \cong A \Delta y_{hkl} \parallel \quad \text{for} \quad \Delta y \text{ small.}$$

The value of  $A$  may be calculated from the equation

$$y = r\zeta / \sqrt{1 - \zeta^2}$$

which expresses the relation between  $y$  and  $\zeta$  for a cylindrical camera of radius  $r$  (Buerger, 1942, p. 141).

The equation for pericline twinning may be rewritten as

$$lc^* \cos \alpha^* + ha^* \cos \gamma^* = \frac{1}{4kb^*} (\xi_{hkl} + \xi_{\bar{h}\bar{k}\bar{l}})(\xi_{hkl} - \xi_{\bar{h}\bar{k}\bar{l}}).$$

If  $\Delta x$  is the displacement between the positions of  $(hkl)$  and  $(\bar{h}\bar{k}\bar{l})$  and

$$\frac{1}{B} = \frac{1}{4kb^*} (\xi_{hkl} + \xi_{\bar{h}\bar{k}\bar{l}}) \left( \frac{dx}{d\xi} \right) \quad \text{at} \quad \xi = \frac{1}{2} (\xi_{hkl} + \xi_{\bar{h}\bar{k}\bar{l}}) \quad \text{and} \quad \zeta = \zeta_{hkl}$$

then

$$lc^* \cos \alpha^* + ha^* \cos \gamma^* \cong \frac{1}{B} \cdot \Delta x_{hkl} \quad \text{for} \quad \Delta x \text{ small.}$$

§ It may be shown that this equation is valid for  $k=0$  even though the derivation is not valid.

|| All approximation signs imply a possible error of about 1% which may be neglected in view of the required accuracy of the method.



$(dx/d\xi)$  may be calculated from the equation

$$x = \frac{2\pi r}{360^\circ} \cos^{-1} \left( \frac{2 - \xi^2 - \xi'^2}{2\sqrt{1 - \xi^2}} \right)$$

(Buerger, 1942, p. 141).

For both albite and pericline twinning, values of  $lc^* \cos \alpha^* + ha^* \cos \gamma^*$  may be obtained. In order to determine  $c^* \cos \alpha^*$  and  $a^* \cos \gamma^*$  the measured values of  $lc^* \cos \alpha^* + ha^* \cos \gamma^*$  are divided by  $h$  and plotted against  $l/h$ . The values should fall on a straight line whose gradient is  $c^* \cos \alpha^*$  and whose intercept at  $l/h=0$  is  $a^* \cos \gamma^*$ .

Tables 1 and 2 and Fig. 5 contain data from which the values of  $A$  and  $B$  may be determined. As  $b^* \simeq 0.120$  throughout the alkali feldspar

TABLE 1. VALUES OF  $A$

Layer line	$\xi$	$A$ for 3 cm. camera	$A$ for $9/\pi$ cm. camera
0	0.00	0.01667	0.01745
1	0.12	0.01650	0.01727
2	0.24	0.01525	0.01596
3	0.36	0.01354	0.01417
4	0.46	0.01125	0.01178
5	0.60	0.00853	0.00893
6	0.72	0.00587	0.00583

series the values of  $A$  are approximately the same for all the alkali feldspars. The values of  $A$  in Table 1 have been calculated for  $b^*=0.120$  and for cameras of radius 3 and  $9/\pi$  cm. Figure 6 contains graphs of  $B$  as a function of  $(\xi_{hkl} + \xi_{\bar{h}\bar{k}\bar{l}})$  for the layer lines 3, 4, 5, and 6. The value 0.120 for  $b^*$  has again been used. Curves for the layer lines 1 and 2 are not given because the accuracy of measurement of these layer lines is insufficient.

The procedure for albite twinning is as follows:

(1) Measure  $\Delta y$  (in mm.) perpendicular to the layer lines for the sets of  $(hkl)$  and  $(\bar{h}\bar{k}\bar{l})$  reflections. Take the average of the two values of  $\Delta y$  obtained for the positive and negative layer lines. The reflections may be indexed by comparison with Fig. 3.

(2) Multiply  $\Delta y$  by  $A$  and divide by the appropriate value of  $h$ .  $A$  may be found from Table 1. If a soda phase is being measured, values of  $A/h$  may be found in Table 3.

(3) Plot the values of  $A\Delta y/h$  against  $l/h$ . Measure the gradient and the intercept at  $l/h=0$ .  $\cos \alpha^* = \text{gradient}/c^*$  and  $\cos \gamma^* = \text{intercept}/a^*$ .

A set of values of  $\Delta y$  for specimen  $O$  is given in Table 3 and has been plotted in Fig. 6. The value of  $A\Delta y/h$  may be either positive or

TABLE 2. DATA FOR THE CONSTRUCTION OF FIGURE 5

$\xi(hkl) + \xi(\bar{h}\bar{k}\bar{l})$	Values of $B$			
	6th layer	5th layer	4th layer	3rd layer
0.25				215.5
0.35				139.1
0.45			164.5	104.3
0.55			126.1	84.7
0.65		159.2	103.6	71.5
0.75	244.6	129.0		
0.85	179.4	110.0	77.4	54.5
0.95	146.7	96.3	69.2	49.0
1.05	125.8	86.1	62.6	44.7
1.15		78.2	57.3	
1.25	100.6	72.0	53.1	38.0
1.65	76.4	56.2	41.9	30.1
2.05	65.3	48.4	36.1	25.8
2.45	62.3	45.2	33.2	23.6
2.85	67.8	46.4	33.2	23.2
3.05	78.7			
3.25	115.2	57.9	37.9	25.4
3.35		66.1		
3.45		82.9	45.3	28.8
3.55			53.6	
3.65			74.2	35.6
3.75				50.2

negative, for no attempt has been made to determine the sign. It is obvious in this case, that to obtain a linear relation the values of  $A\Delta y/h$  for  $l/h$  negative must have an opposite sign from those with  $l/h$  positive. In triclinic crystals the interaxial angles may be taken arbitrarily as greater or less than  $90^\circ$ . For albite it is customary to take  $\alpha^*$  less than  $90^\circ$  and for microcline it is customary to take  $\alpha^*$  greater than  $90^\circ$ , which relations may be obtained by taking  $A\Delta y/h$  negative for negative values of  $l/h$ . The values  $a^*=0.211$  and  $c^*=0.242$  may be used for the soda phase of an alkali feldspar, since low-albite (composition  $Ab_{100}$ ) has values of 0.2109 and 0.2413, high-albite ( $Ab_{100}$ ) has 0.2109 and 0.2424 and a high-temperature feldspar of composition  $Or_{10}Ab_{90}$  has 0.2100 and 0.2418, which values do not deviate by more than 1% from the chosen values. The values  $a^*=0.200$  and  $c^*=0.238$  may be used for microcline. For specimen  $O$ ,  $\alpha^*=86^\circ 43'$ ,  $\gamma^*=90^\circ 15'$  from the gradient and intercept of Fig. 7.

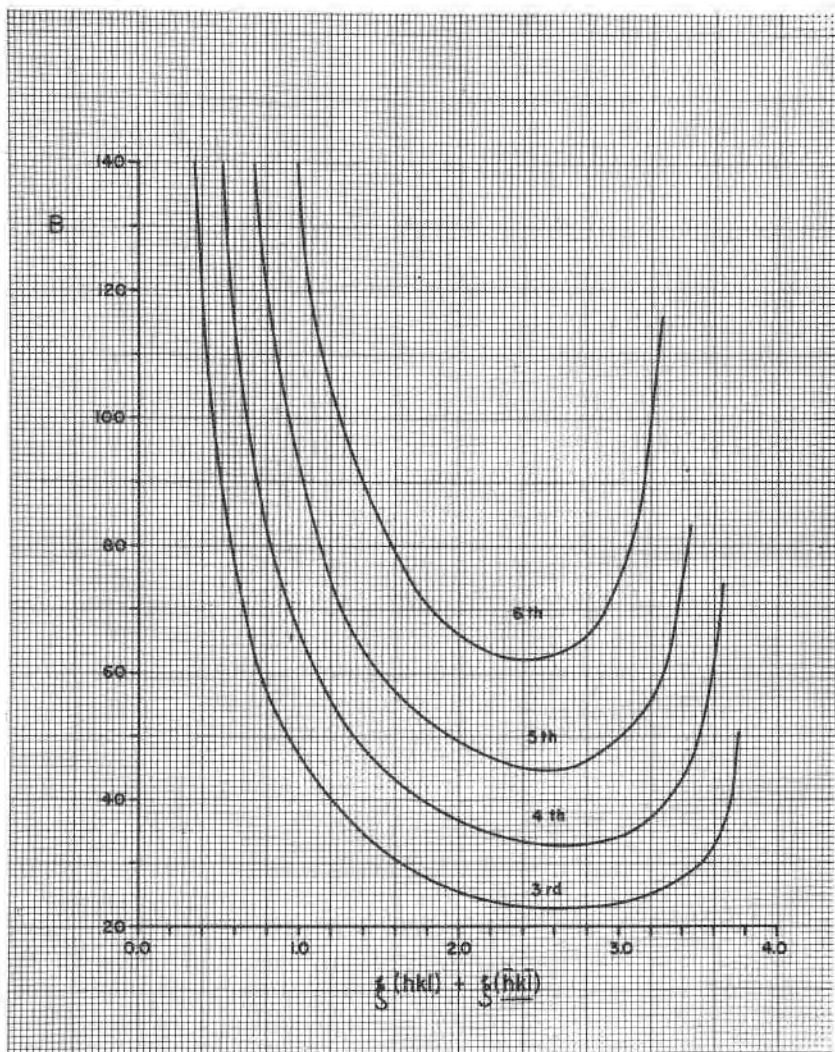


FIG. 5.  $B$  as a function of  $(\xi_{hkl} + \xi_{\bar{h}\bar{k}l})$  for the 3rd, 4th, 5th and 6th layer lines with  $\delta^* = 0.120$ . The values have been calculated for a cylindrical camera of radius 3 cm. To obtain values of  $B$  for a camera of radius  $9/\pi$  cm. multiply the value of  $B$  obtained from the diagram by  $3/\pi$ . The data for construction of the diagram are set down in Table 2.

The procedure for pericline twinning is as follows:

(1) Measure  $\Delta x$  in mm. Take the average of the two values of  $\Delta x$  obtained for the positive and negative layer lines. The reflections may be indexed by comparison with Fig. 3.

TABLE 3. ALBITE TWINNING OF SPECIMEN O

$hkl$	$l/h$	$\Delta y$ (mm.)	$A\Delta y/h$	$A/h$ 3 cm. camera	$A/h$ $9/\pi$ cm. camera
66 $\bar{5}$ *	-0.833	14.3	0.01327	.000928	.000972
46 $\bar{4}$	-1.0	10.9	0.01517	.001392	.001457
26 $\bar{2}$ *	-1.0	5.25	0.01462	.002785	.002915
55 $\bar{5}$	-1.0	8.95	0.01527	.001706	.001786
35 $\bar{4}$	-1.333	7.0	0.01990	.002843	.002977
44 $\bar{5}$ *	-1.25	6.65	0.01870	.002812	.002945
24 $\bar{3}$	-1.5	3.9	0.02194	.005625	.005890
24 $\bar{2}$ *	1.0	2.25	0.01266	.005625	.005890
44 $\bar{2}$ *	0.5	2.10	0.00590	.002812	.002945
33 $\bar{5}$	-1.667	5.15	0.02324	.004513	.004723
13 $\bar{2}$	-2.0	2.00	0.02708	.01354	.01417
13 $\bar{2}$ *	2.0	1.95	0.02640	.01354	.01417
33 $\bar{2}$ *	0.667	1.80	0.00812	.004513	.004723
42 $\bar{5}$	-1.25	4.8	0.01830	.003812	.003990
22 $\bar{4}$ *	-2.0	3.7	0.02821	.007625	.007980
22 $\bar{2}$ *	1.0	1.55	0.01182	.007625	.007980
40 $\bar{6}$	-1.5	5.25	0.02188	.004167	.004362
20 $\bar{4}$ *	-2.0	3.6	0.03000	.008333	.008725
20 $\bar{2}$	1.0	1.55	0.01292	.008333	.008725
20 $\bar{3}$ *	1.5	2.4	0.02000	.008333	.008725
40 $\bar{2}$	0.5	1.6	0.00667	.004167	.004362

Measurements were made on a camera of radius 3 cm.

\* Most suitable reflections.

TABLE 4. PERICLINE TWINNING OF SPECIMEN O

$hkl$	$l/h$	$\frac{\xi hkl + \xi \bar{h}\bar{k}\bar{l}}{\xi \bar{h}\bar{k}\bar{l}}$	$\Delta x$ (mm.)	$\Delta x/Bh$	$Bh$ 3 cm. camera	$Bh$ $9/\pi$ cm. camera
461	0.25	1.96	—		271	249
26 $\bar{2}$	-1.0	0.95	4.1	0.01385	296	283
46 $\bar{4}$	-1.0	1.91	3.9	0.01444	270	258
66 $\bar{5}$	-0.833	2.60	—		380	363
35 $\bar{2}$	0.667	1.93	—		154	147
35 $\bar{4}$	-1.333	1.91	2.97	0.01967	151	144
55 $\bar{5}$	-1.0	2.395	3.27	0.01441	227	217
641	0.167	2.79	—		198	189
24 $\bar{3}$	-1.5	1.305	2.27	0.02204	103	98
24 $\bar{2}$	1.0	1.55	1.07	0.01216	88	84
44 $\bar{2}$	0.5	2.31	0.87	0.00640	136	130
13 $\bar{2}$	-2.0	0.86	1.55	0.02844	54.5	52
33 $\bar{5}$	-1.667	2.16	1.8	0.02432	74	70.7
13 $\bar{2}$	2.0	1.22	—		38.7	37
33 $\bar{2}$	0.667	1.93	0.65	0.00788	82.5	78.8

Measurements were made on a 3 cm. camera. The reflections for which  $\Delta x$  is not recorded will be found useful if a high-temperature feldspar is measured.

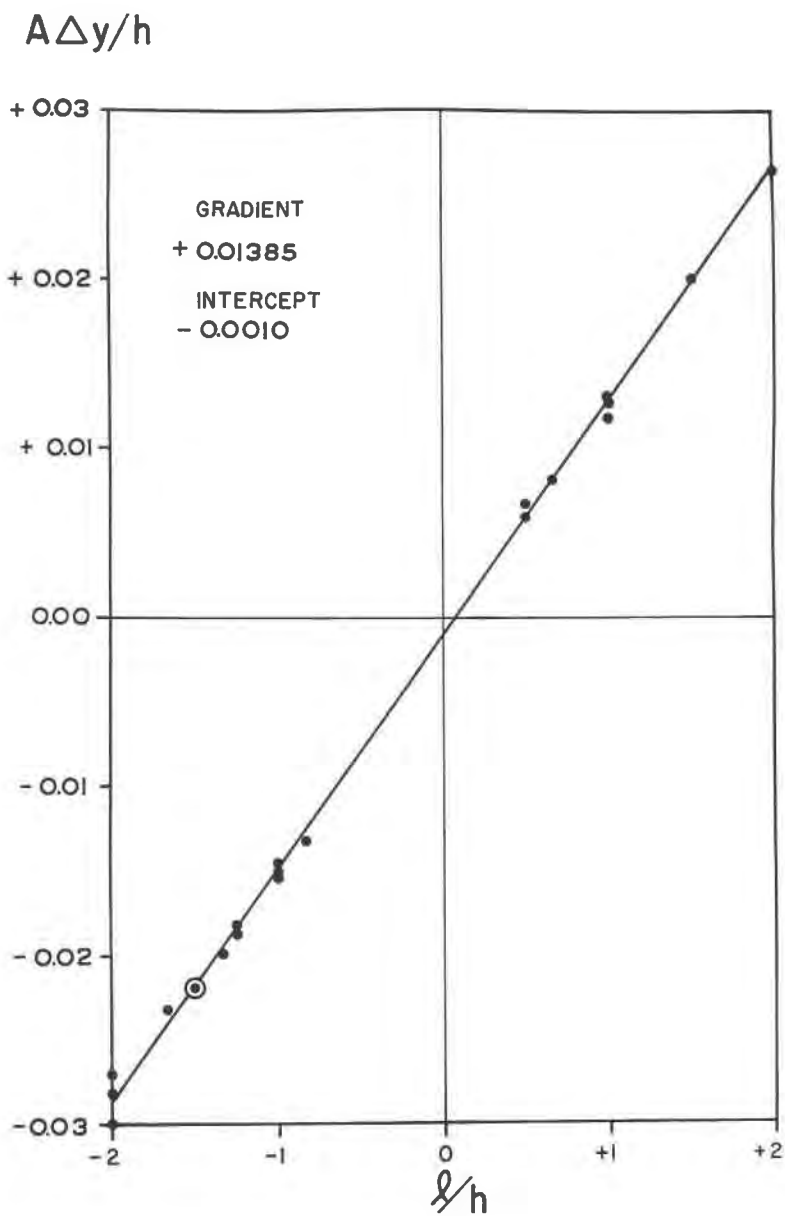


FIG. 6. A graph of  $A\Delta y/h$  versus  $l/h$  for values of  $\Delta y$  taken from the albite-twinned soda phase of specimen *O*. The data are set out in Table 3.

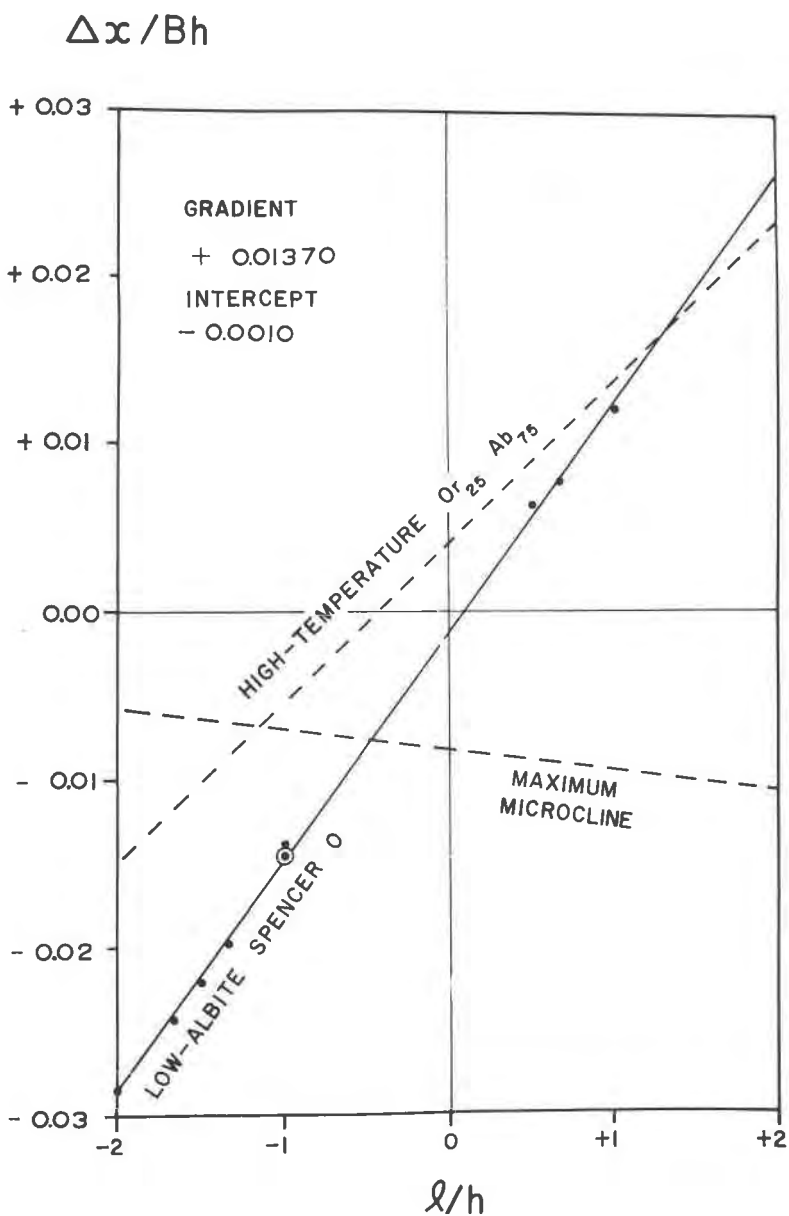


FIG. 7. A graph of  $\Delta x/Bh$  versus  $l/h$  for values of  $\Delta x$  taken from the pericline-twinned soda phase of specimen *O*. The data are set out in Table 4. All low-albite phases will give values close to those for specimen *O*. For comparison the lines relating  $(c^* \cos \alpha^* + a^* \cos \gamma^*)$  with  $l/h$  for a maximum microcline and for a high-temperature alkali feldspar of composition near  $Or_{26}Ab_{75}$  are also shown. The lattice angles of the microcline have been taken as  $\alpha^* = 90^\circ 18'$ ,  $\gamma^* = 92^\circ 22'$ , and for the high-temperature alkali feldspar the values  $\alpha^* = 87^\circ 44'$ ,  $\gamma^* = 88^\circ 52'$  have been used.

Steps 2 and 3 may be omitted if a soda phase is being measured, since values of  $Bh$  for the most suitable reflections are given in Table 4. If a potash phase is being measured the procedure is:

- (2) Measure  $\xi_{hkl}$  and  $\xi_{\bar{h}\bar{k}\bar{l}}$  using a Bernal chart.
- (3) From the appropriate curve in Fig. 5 determine the value of  $B$  for  $\xi = (\xi_{hkl} + \xi_{\bar{h}\bar{k}\bar{l}})$ .
- (4) Divide  $\Delta x$  by  $Bh$ .
- (5) Plot the values of  $\Delta x/Bh$  against  $l/h$ . Further steps are identical with those for the albite twinning.

A set of values of  $\Delta x$  for specimen *O* is given in Table 4 and plotted in Fig. 7. They give  $\alpha^* = 86^\circ 45'$  and  $\gamma^* = 90^\circ 15'$ .

The accuracy obtainable from the method depends, of course, on the quality of the  $x$ -ray reflections and the number of measurements. In general, it has been found that an accuracy between  $3'$  and  $10'$  of arc is obtainable from most photographs. The measurement and calculation of  $\alpha^*$  and  $\gamma^*$  for one pair of twinned individuals takes about 30 minutes.

We are indebted to Drs. Spencer, Bowen, and Tuttle for the opportunity to use the three specimens for which  $x$ -ray photographs are given in this paper. Drs. J. D. H. and G. Donnay critically reviewed the manuscript and we are grateful to them for their suggestions.

#### REFERENCES

- BOWEN, N. L., & TUTTLE, O. F. (1950): The system  $\text{NaAlSi}_3\text{O}_8$ — $\text{KAlSi}_3\text{O}_8$ — $\text{H}_2\text{O}$ : *Jour. Geol.*, **58**, 489–511.
- BUERGER, M. J. (1942): *X-ray Crystallography*, John Wiley & Sons, Inc., New York.
- CHAO, S. H., & TAYLOR, W. H. (1940): The lamellar structure of potash-soda feldspars: *Proc. Roy. Soc., Ser. A*, **174**, 57–72.
- HENRY, N. F. M., LIPSON, H., & WOOSTER, W. A. (1951): *The Interpretation of X-ray Diffraction Photographs*, Macmillan & Co., London.
- LAVES, F. (1952): Phase relations of the alkali feldspars: *Jour. Geol.*, **60**, 436–450, 549–574.
- SPENCER, E. (1937): The potash-soda-feldspars. I. Thermal stability: *Mineral. Mag.*, **24**, 453–494.

*Manuscript received July 22, 1954*